Supporting Information

Density Functional Theory +U Analysis of the Electronic Structure and Defect Chemistry of LSCF ($La_{0.50}Sr_{0.50}Co_{0.25}Fe_{0.75}O_{3-\delta}$)

Andrew M. Ritzmann,[1] Johannes M. Dieterich,[2] and Emily A. Carter[2,3]

[1]Department of Chemical and Biological Engineering, [2]Department of Mechanical and Aerospace Engineering, and [3]Program in Applied and Computational Mathematics and the Andlinger Center for Energy and the Environment, Princeton University, Princeton, NJ 08544-5263, United States

Contents:

S1. Analysis of the Electronic Structure of $La_{0.50}Sr_{0.50}CoO_3$

We analyzed the electronic structure of $La_{0.50}Sr_{0.50}CoO_3$ (LSC) using Kohn-Sham density functional theory (KS-DFT)[1,2] calculations. Unlike many of the SOFC materials we have investigated (*e.g.*, LSCF, $La_{0.50}Sr_{0.50}Co_{0.25}Fe_{0.75}O_3$, from the main article text), LSC is metallic.[3] We performed traditional DFT calculations on LSC within the generalized gradient approximation (GGA) to electron exchange and correlation (XC).[4] Since many transition metal (TM) oxides of this form require the DFT+U method[5] to correct for spurious self-interaction errors,[6,7] we also analyzed LSC using DFT+U calculations. Our goal is to determine which method gives a better description of the electronic structure of LSC.

Since metallic LSC is different than the semiconducting LSCF encountered in the main text, we will provide computational details for our analysis. The calculations were performed with the 2 × 2 × 2 supercell (pseudocubic, figure S1) of the cubic perovskite structure. For simplicity, we restrict our discussion to the cell with an isotropic distribution of La/Sr ions as depicted in figure S1. We employed the Vienna Ab initio Simulation Package (VASP) version

5.2.2 for our spin-polarized DFT and DFT+U calculations.[8–10] The DFT+U calculations were performed with the rotationally invariant formulation of Dudarev *et al.*[11] with U_{eff} = U-J = 4 eV for the Co 3*d* orbitals. This value of U_{eff} was derived from electrostatically embedded unrestricted Hartree-Fock calculations for Co^{3+} in $LaCoO_3$.[6] We employed the XC functional of Perdew, Burke, and Ernzerhof (PBE).[4] The pseudocubic structures were optimized by allowing the cell volume to change and the nuclei to find their lowest energy arrangement, subject to the constraint that the cell remained cubic. The structures were considered converged when the external pressure was below 0.05 kBar and the force on each nucleus was below 0.03 eV/Å. Integration over the first Brillouin zone was performed with first-order Methfessel-Paxton[12] smearing (σ = 0.20 eV) during structural relaxations and the tetrahedron method with Blöchl corrections[13] for single point calculations thereafter. The electronic entropy was below 5 meV/ f.u. during the relaxations. A 4 × 4 × 4 Monkhorst-Pack k-point mesh was employed.[14] The planewave kinetic energy cut-off was set at 750 eV. These parameters ensured that the total energy was converged to 5 meV/f.u. The projector augmented-wave (PAW) method[15] was employed to represent the interactions between the valence electrons and the nuclei plus core electrons. The PAW potentials were taken from the VASP library[16] and were as follows: Co ($4s^2 3d^7$), La ($5s^2 5p^6 6s^2 5d^1$), Sr_sv ($4s^2 4p^6 5s^2$),[a] and 'regular' O ($2s^2 2p^4$). Bader charge analysis was performed using the code from Prof. Graeme Henkelman's group at the University of Texas.[17–19]

[a] The Sr_sv label for the strontium PAW potential indicates that the semi-core electrons (4*s* and 4*p* manifolds) are explicitly treated as valence electrons in the calculation.

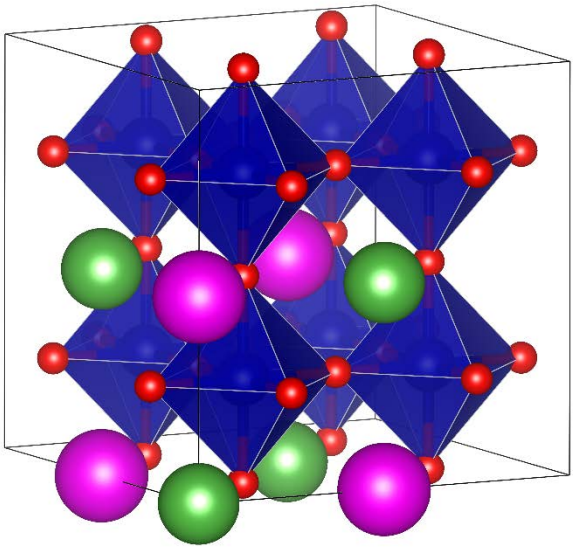

Fig S1 The pseudocubic structure used for modelling LSC. Colour designations: Blue (Co), O (red), La (green), and Sr (pink).

The results of our electronic structure analysis are presented in table S1 and figure S2. We find that both computational methods properly predict metallic behavior for LSC; however, the DFT+U method gives disparate Co magnetic moments.

Table S1. Crystal and electronic structure properties of LSC obtained from DFT-GGA and DFT+U calculations. Appropriate experimental values are provided for comparison. Equilibrium volumes (V_0 in Å^3/f.u.), pseudocubic lattice constants (a_{pc} in Å), Bader charges (q_{La}, q_{Sr}, q_{Co}, and q_O in *e*), and Co magnetic moments (μ_{Co} in μ_B) for LSC (x_{Sr}= 0.50) in the pseudocubic cell with isotropic La/Sr arrangements (figure S1).

	Experiment	DFT-GGA	DFT+U
V_0	54.64[20]	56.6	58.6
a_{pc}	7.59[a]	7.68	7.77
q_{La}	----	2.10	2.10
q_{Sr}	----	1.59	1.59
q_{Co}	----	1.39	1.53 (×6) 1.39 (×2)
q_O	----	-1.08	-1.11 ± 0.03
μ_{Co}	1.8 [21]	1.62-1.64	2.8 (×6) 2.1 (×2)

[a] The pseudocubic lattice constants were derived by doubling the cube-root of the equilibrium volume (per formula unit). This gives a lattice constant that can properly be compared to our data.

The PDOS from the DFT+U calculation is half-metallic with a gap in the β-spin channel. These features result from the DFT+U method attempting to force integer occupations in the Co 3*d* manifold. Our data thus show that the +U correction leads to unphysical electron localization in LSC. On the other hand, the DFT-GGA calculations perform very well for LSC. The Co magnetic moments remain essentially homogeneous, and the PDOS shows that a fully metallic system has developed. DFT-GGA values are consistent with experimental measurements of μ_{Co} in $La_{0.50}Sr_{0.50}CoO_3$, which found a value of 1.8 μ_B.[21] A large peak in the β-spin PDOS at the Fermi level agrees with previous DFT-GGA calculations on LSC.[21] Based on these results, we will use DFT-GGA exclusively in the following discussion of LSC.

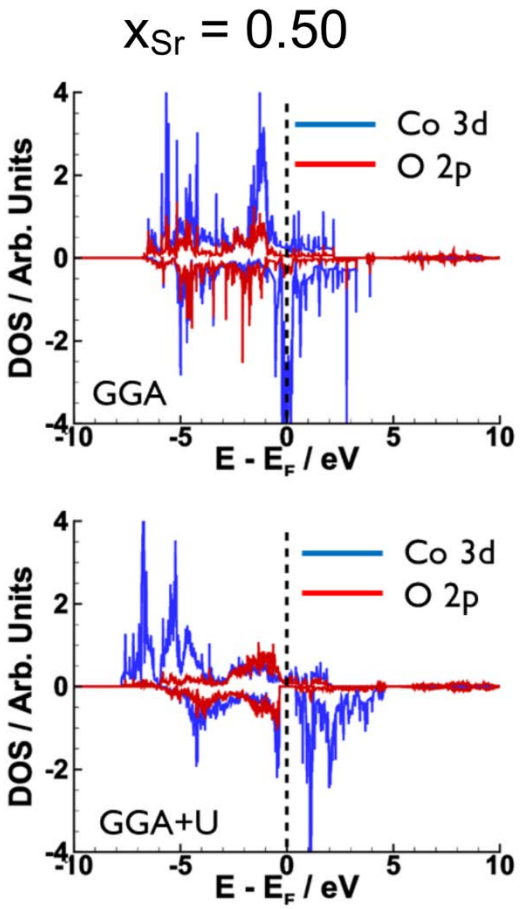

Fig S2 DFT-GGA (top) and GGA+U (bottom) PDOS for LSC (x_{Sr}=0.50) in the pseudocubic cell with isotropic La/Sr arrangements (figure S1). Positive (negative) values refer to α(β)-spin channels.

S2. Analysis of Oxygen Vacancy Formation in $La_{0.50}Sr_{0.50}CoO_3$

Our analysis of oxygen vacancy ($V_O^{\cdot\cdot}$) formation in LSC involved re-optimizing the nuclear positions after removing a single, neutral oxygen atom. As in the main text, we focus on the $V_O^{\cdot\cdot}$ formation energy ($\Delta E_{f,vac}$) in order to understand how readily $V_O^{\cdot\cdot}$ defects form in LSC. $\Delta E_{f,vac}$ is calculated according to equation S1 (also equation 2 in the main text).

$$\Delta E_{f,vac} = E_{defective} + \frac{1}{2}E_{O_2} - E_{host} \quad \text{(S1)}$$

In order to avoid spurious vacancy-vacancy interactions, we employ a larger, 80-atom cell (figure S3) generated by the special quasirandom structures method. This cell contains a distribution of La/Sr ions that mimics the pair correlation functions for first- and second-nearest neighbors. We obtain a value of $\Delta E_{f,vac}$ = 1.25 eV for an oxygen vacancy in the SQS cell surrounded by four La ions.

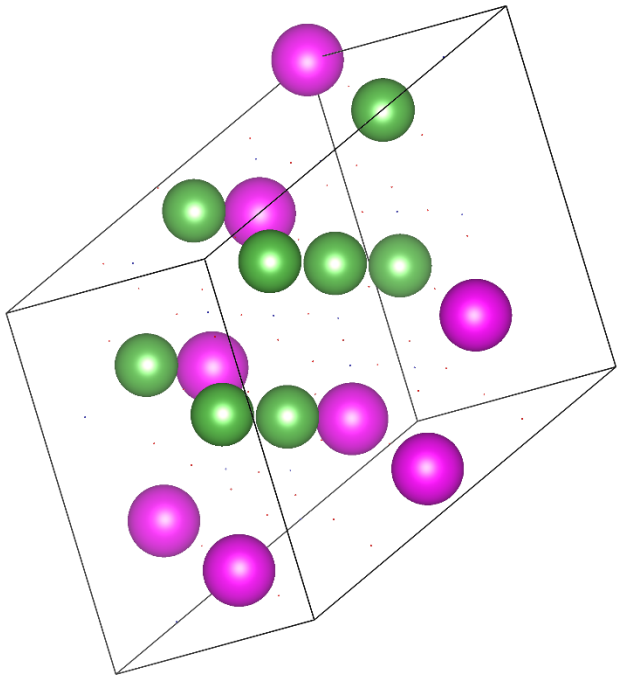

Fig S3 The 80-atom SQS cell with the La/Sr distribution matching first- and second-nearest neighbor correlation functions for a perfectly random alloy. The Co and O atoms are omitted so that the La/Sr distribution can be clearly seen.

In order to further analyze the process of $V_O^{\cdot\cdot}$ formation in LSC, we report the Bader charges with and without the $V_O^{\cdot\cdot}$ present. Using equation S2 (also equation 7 from the main text), we can quantify the extent to which the Bader analysis assigns the excess electrons left behind upon $V_O^{\cdot\cdot}$ formation to the oxygen sublattice.

$$\lambda = \frac{(N-1)(\langle q_{O,nonstoichiometric}\rangle - \langle q_{O,stoichiometric}\rangle)}{\langle q_{O,stoichiometric}\rangle} \quad \text{(S2)}$$

In equation S2, λ is the degree of delocalization, *N* is the number of oxygen ions in the perfect supercell, $\langle q_{O,nonstoichiometric} \rangle$ is the average Bader charge for an oxygen ion in the defective supercell, and $\langle q_{O,stoichiometric} \rangle$ is the average Bader charge for an oxygen ion in the perfect supercell. We note that λ shows significant sensitivity to truncation or rounding of the Bader charges. Our calculation for λ was done without truncation, thus it is more accurate than the value computed by taking our reported Bader charges (rounded to the nearest 0.01 *e*) and substituting them into equation S2. We find that λ = 0.37 for LSC, and we would expect this to correspond to a relatively high value for $\Delta E_{f,vac}$.[22] In fact, we see a relatively high $\Delta E_{f,vac}$ when compared with the value we previously reported for the similar compound $La_{0.50}Sr_{0.50}FeO_3$ ($\Delta E_{f,vac}$ = 0.31 eV). The data presented here show how we obtained the λ and $\Delta E_{f,vac}$ values for LSC found in figure 6 of the main text.

Table S2 Bader charges (q_{La}, q_{Sr}, q_{Co}, and q_O in *e*) for stoichiometric and nonstoichiometric LSC obtained from DFT-GGA calculations in the pseudocubic cell with isotropic La/Sr arrangements (figure S1). Co* refers to a Co site adjacent to an oxygen vacancy. Uncertainties are plus/minus one standard deviation.

	x_{Sr}=0.50	
	Without $V_O^{\cdot\cdot}$	**With $V_O^{\cdot\cdot}$**
q_{La}	2.09	2.09
q_{Sr}	1.60	1.59
q_{Co}	1.41 ± 0.01	1.37 ± 0.01
q_{Co*}	----	1.27
q_O	-1.08 ± 0.01	-1.09 ± 0.02

S3. References

1 P. Hohenberg and W. Kohn, *Phys. Rev.*, 1964, **136**, B864–B871.

2 W. Kohn and L. J. Sham, *Phys. Rev.*, 1965, **140**, A1133–A1138.

3 A. Mineshige, M. Inaba, T. Yao, Z. Ogumi, K. Kikuchi and M. Kawase, *J. Solid State Chem.*, 1996, **121**, 423–429.

4 J. P. Perdew, K. Burke and M. Ernzerhof, *Phys. Rev. Lett.*, 1996, **77**, 3865–3868.

5 V. I. Anisimov, J. Zaanen and O. K. Andersen, *Phys. Rev. B*, 1991, **44**, 943–954.

6 A. M. Ritzmann, M. Pavone, A. B. Muñoz-García, J. A. Keith and E. A. Carter, *J. Mater. Chem. A*, 2014, **2**, 8060–8074.

7 A. M. Ritzmann, A. B. Muñoz-García, M. Pavone, J. A. Keith and E. A. Carter, *Chem. Mater.*, 2013, **25**, 3011–3019.

8 G. Kresse and J. Hafner, *Phys. Rev. B*, 1993, **48**, 13115–13118.

9 G. Kresse and J. Furthmüller, *Phys. Rev. B*, 1996, **54**, 11169–11186.

10 G. Kresse and J. Furthmüller, *Comput. Mater. Sci.*, 1996, **6**, 15–50.

11 S. L. Dudarev, G. A. Botton, S. Y. Savrasov, C. J. Humphreys and A. P. Sutton, *Phys. Rev. B*, 1998, **57**, 1505–1509.

12 M. Methfessel and A. T. Paxton, *Phys. Rev. B*, 1989, **40**, 3616–3621.

13 P. E. Blöchl, O. Jepsen and O. K. Andersen, *Phys. Rev. B*, 1994, **49**, 16223–16233.

14 H. J. Monkhorst and J. D. Pack, *Phys. Rev. B*, 1976, **13**, 5188–5192.

15 P. E. Blöchl, *Phys. Rev. B*, 1994, **50**, 17953–17979.

16 G. Kresse and D. Joubert, *Phys. Rev. B*, 1999, **59**, 1758–1775.

17 R. F. W. Bader, *Atoms in Molecules: A Quantum Theory*, Oxford University Press, USA, New York, 1994.

18 G. Henkelman, A. Arnaldsson and H. Jónsson, *Comput. Mater. Sci.*, 2006, **36**, 354–360.

19 W. Tang, E. Sanville and G. Henkelman, *J Phys Condens Matter*, 2009, **21**, 084204.

20 V. G. Sathe, A. V. Pimpale, V. Siruguri and S. K. Paranjpe, *J. Phys. Condens. Matter*, 1996, **8**, 3889–3896.

21 R. P. Haggerty and R. Seshadri, *J. Phys. Condens. Matter*, 2004, **16**, 6477–6484.

22 A. B. Muñoz-García, A. M. Ritzmann, M. Pavone, J. A. Keith and E. A. Carter, *Acc. Chem. Res.*, 2014, **47**, 3340–3348.